Comparison of Force and Power Generation Patterns and their Predictions under Different External Dynamic Environments

Pratik Y. Chhatbar, *Student Member, EMBS, IEEE* and Joseph T. Francis

Abstract—Use of neural activity to predict kinematic variables such as position, velocity and direction etc of movements has been implemented in real-time control of robotic systems and computer cursors. In everyday life, however, we generate variable amounts of force to manipulate objects of different inertial properties or to follow the same trajectory under different external dynamic environments like air or water. The resultant work during such movements, and its time derivative power, should depend on the dynamics of the movement. In order to give the users of a brain-machine interface (BMI) comprehensive control of a prosthetic limb under different dynamic conditions, it is imperative to consider the dynamics-related parameters like end-effector forces, joint torques or power. In this paper, we show distribution patterns of two such dynamics parameters – force and power – and their predictive efficiency under different dynamic environmental conditions. We intend to find the force-related parameter, which has optimal predictive efficiency across different dynamic environments that is generalization. Our ultimate goal is to materialize a force-based brain-machine interface (fBMI).

Index terms—Brain-Computer Interface, Power, Force-related Parameters, Robotic Manipulandum, Chronic Microelectrode Array, Motor Learning, Reaching Movements, Neuroprosthetics

I. INTRODUCTION

OVER the past decade several groups have shown neural activity recorded from the motor cortex can be used to control a brain-machine interface (BMI). At present all BMIs have allowed the user to control kinematic variables such as end-point/joint position or velocity. Such kinematic control may be useful for a BMI, but it is clearly different from the type of control we use on a daily basis, changing the output forces we use as a function of the situation, such as when picking up a full vs. an empty cup of coffee. It is easy to imagine how such dynamic related control may lead to a more natural feeling BMI controller. Neural prostheses have been able to predict discrete [1-2] and continuous [3-7] behavioral data from neural signals. In addition researchers have generated learning based decoders [8-9]. Efforts have been made to include force into such work [10-11], but little is known of how well a neural decoder trained under one force-field environment could generalize to novel force-field environment.

To predict the generated force-related parameters, we used multiple linear regression models fed with the first 20 principal components calculated from neural activity recorded from hundreds of motor cortex neurons while the monkey worked on a center-out reaching task. Reaching movements were made using a block paradigm with blocks of either a high or a low gain viscous force-field. Our results show that when we train our models to predict the power and force in a low gain viscous force-field environment, they predict these variables approximately as well under a high gain viscous force-field environment or even better, but the opposite tends to be false, except for when looking at power. We hope that by combining such generalization of power, we can provide better and more natural control of a BMI.

II. METHODS

A. Subjects and Behavioral Task

All animal handling and experimental procedures were approved by IACUC of SUNY Downstate Medical Center and are assisted and scrutinized by Division of Laboratory Animal Resources at SUNY Downstate Medical Center. A female Bonnet Macaque (*M. radiata*) (Age 10 years, weight 4.5 kg) was trained under a modified 8-target center-out reaching task, where she had to perform the task under cycling blocks of 10 consecutive trials in a low (3 Ns/m) followed by 10 high (12 Ns/m) end-point viscous force field. A KINARM setup for non-human primates [12] was used for the behavioral task.

B. Microelectrode Arrays and Implantation Procedure

Three floating microelectrode arrays [13-14] of 10x10 Iridium Oxide coated electrodes of 1.5 mm lengths (Blackrock Microsystems, Salt Lake City, UT) were implanted in primary motor cortex (M1), primary somatosensory cortex (S1) and dorsal premotor cortex (PMd), only M1 results are described in this paper. The

Pratik Y. Chhatbar is a graduate student at SUNY Downstate Medical Center Physiology and Pharmacology Department under joint mentorship of Dr. Joseph T. Francis and John K. Chapin. He is working towards his Ph.D. degree in joint Graduate Program in Biomedical Engineering between SUNY Downstate Medical Center and Polytechnic Institute of New York University at Brooklyn, NY 11203 (e-mail: pratik.chhatbar@downstate.edu, pratikchhatbar@gmail.com).

Dr. Joseph T. Francis is an Assistant Professor at Physiology and Pharmacology Department, and holds faculty position in Graduate Program in Neurobiology and behavior, SUNY Downstate Medical Center, Brooklyn, NY 11203 and is also faculty and executive committee member in joint Graduate Program in Biomedical Engineering between SUNY Downstate Medical Center and Polytechnic Institute of New York University. (phone: 718-270-6338; fax: 718-270-3103; e-mail: joe.francis@downstate.edu, joey199us@gmail.com).

implantation site spanned the shoulder region as confirmed by intra-operative single electrode recordings from S1. Details of surgical implantation technique and use of our Nesting Platform (NP) to hold multiple connectors from the arrays has been previously described [15]. A few months before implantation a headpost implantation surgery was performed [16] to restrict head movements while the
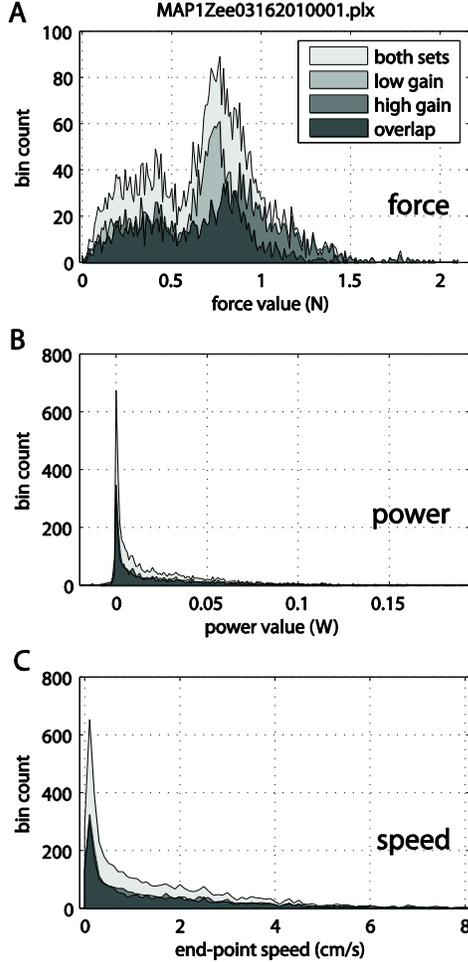

Fig. 1. Distribution patterns of monkey-generated force magnitude (A), power (B) and speed (C) under low-gain (light gray) and high-gain (dark gray) viscous field. The overlap of the distribution is demarked by darker shade, and lightest gray represent the total distribution through the entire task consisting of the mixture of low- and high-gain viscous environments. Note the highly separate distribution patterns of force generation under different viscous field conditions, which is not the case power or speed profiles.

monkey performed the task.

C. Neural Recordings

Neural signals were high-pass filtered, differentially referenced, amplified and thresholded as per individual characteristics of that electrode channel and sampled at 40 KHz. Online spike sorting was used to pick off putative single unit activity, all spike timestamps and waveform data were saved for further offline analysis [17]. As the monkey performed the center-out reaching task, kinematic variables (joint positions, velocities, accelerations) and applied

torques at each joint where recorded. Muscle activities were recorded through surface EMG leads after shaving the skin contact areas and applying conductive gel on the leads.

D. Data Processing and Analysis

Before processing the data in the offline case the recorded waveforms are sorted using Offline Sorter (Plexon Inc., Dallas, TX) using an automatic Valley Seeking algorithm [18]. Matlab (Mathworks Inc., Natick, MA) was then used for all data analysis. We used 100 ms bins and neural activity from 10 bins in the past (total 1 second) for all analysis. Each of the binned neural spiking data and behavioral data were then Z-score transformed. We used multiple linear regression coefficients fit to the data to filter the incoming neural data [4], and found in our experimental setup that the neural activity of M1 recordings gave the best prediction values when using the first 20 principal components of the combined neural signals. Thus we will concentrate our further discussion only on M1 recordings. The general form of such a model is described below:

$$\hat{y}(T) = b + \sum_{i=1}^{m} \sum_{t=1}^{n} (\alpha_i \Sigma t * M_i(T - t)) \qquad (1)$$

where $\hat{y}$ is the predicted variable of interest (e.g., power, force) at time T; b is the y-intercept, $\alpha_i(t)$ are the filter coefficients for the M_i's that represent the score of the ith principal component at time bins $T - t$ (we used $n = 10$ and $m = 20$ as described above). The transformation of neural activity space to principal component space is described in matrix notation by:

$$M_{(1xn)}(T) = N_{(1xn)}(T)\ C_{(nxn)} \qquad (2)$$

where $M_{(1xn)}$ is the vector of principal component scores for a given time bin T; $N_{(1xn)}$ is the vector of normalized neural spike counts on each unit for the same time bin T, and $C_{(nxn)}$ is the principal component coefficient matrix.

Calculation of power is done by first working on the inverse dynamics of the system [12, 19]. The inertial properties of limb segments were estimated from the weight of the monkey and limb segment lengths [20], and those of the robotic systems were made available by the company that commercializes KINARM (BKin Technologies, Kingston, ON, Canada). The generalized form of such inverse dynamics equation can be described as:

$$\tau_{mon} = M(\theta, \dot{\theta}, \ddot{\theta}) + C(\theta, \dot{\theta}) + G(\theta) - \tau_{cmd} - \tau_{frc} \quad (3)$$

where τ_{mon} is torque generated by the monkey (with separate shoulder and elbow components), M is the inertial matrix of the whole system, C is the term for coriolis and centripetal forces, G is the gravity term (which will be 0 in our case because of planar nature of manipulandum performing movements about horizontal plane). $\theta, \dot{\theta}, \ddot{\theta}$ denote joint (in our case, shoulder and elbow) angular positions, velocities and accelerations, respectively. τ_{cmd} is the commanded torques by attached motors in order to create the virtual environment and τ_{frc} is the friction torques generated inside the torque motors as the monkey makes the movements. The negative sign before the last two terms is because the monkey has to overcome those torque values in order to make the movements.

We used these torque values to calculate the power,

$$P = \tau_{sh}\dot{\theta}_{sh} + \tau_{elb}\dot{\theta}_{elb} \tag{4}$$

where P is the power generated by monkey which is a linear summation of power generated at the shoulder and elbow, each of which can be calculated by the torque generated at each joint multiplied by the angular velocity of the joint.

Another way to calculate the power is to first transform the joint torques into end-point forces using the generalized formula,

$$\vec{\tau} = \vec{l} \times \vec{F} \tag{5}$$

where $\vec{\tau}$ is the joint torque vector, $\vec{F}$ is the end-point force vector, $\vec{l}$ is the vector joining the points where torque and force are applied. 'x' denotes cross/vector product. The end-point force can then be used to calculate the power as below:

$$P = \vec{F} \cdot \vec{v} \tag{6}$$

which is dot/scalar product of end-point force vector and end-point velocity vector. Note here that the power calculated by equations (4) or (6) use Polar or Cartesian coordinate frame respectively, and that the difference between these two equations is purely cosmetic. In our calculations, we found no difference in power calculated by either of these equations (R>0.99).

III. RESULTS AND DISCUSSION

It is knows how neural activity patterns change under loads at different joints and postures [21-22]. This suggests that limb motor control is accomplished via a group of separable controllers running in parallel, such that the existence of multiple internal models is supported. Results from bimanual tasks lead to similar conclusions [23-24]. It has been about two decades since neural population vectors have been shown to deferrer between external static and dynamic forces [25] as well as for power and kinematic variables such as position [26-27]. It has been shown that both M1 and PMd, previously thought of as regions of execution and planning respectively, can both contribute

equally well to the predictions of force-related variables [28]. Here we try to address two questions. First, whether we
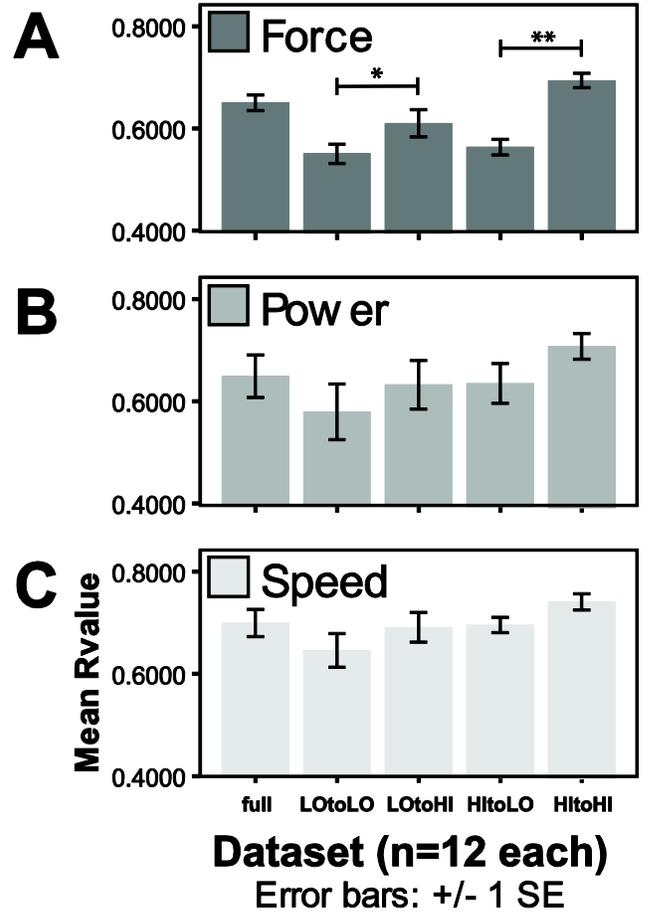

Fig. 2. Comparison of prediction correlation coefficients trained under one gain field environment and tested under same or another gain viscous field environment. Shown here are results on force (A), power (B) and speed (C) from 12 datasets. *Full*-model trained from the mixed data consisting of both low- and high-gain viscous field environments to predict the variable under same mixed environments. *LOtoLO*-model trained in low-gain environment to predict in low-gain environment. *LOtoHI*-model trained in low-gain environment to predict in high-gain environment. *HItoLO*-model trained in high-gain environment to predict in low-gain environment. *HItoHI*-model trained in high-gain environment to predict in high-gain environment. Note that force predictions differ when the model trained under one gain field environment is used to predict in different gain field environment (post-hoc t-test; *p<0.05, **p<0.001). Statistically we failed to find the difference between predictive efficiency of power or speed values for models that are trained under various viscous environments and tested on the others(ANOVA).

can generalize our assumptions of motor control under different external dynamic environmental conditions. Secondly, under such conditions which parameter of motion will make the most consistent candidate for the control of a BMI.

We found comparable speed profiles under two viscous gain field conditions (-3 Ns/m and -12 Ns/m gains on end-point velocity) suggesting that the monkey's task performance was similar under both conditions (see Fig. 1(C)). The forces generated by the monkey under high-gain field conditions were increased, explaining the maintenance of such comparable speed profiles (see Fig. 1(A)). However,

the distribution of monkey-generated power, which is displacement per unit time multiplied by the force component in the direction of displacement, remained similar under both gain field conditions. With these findings we believe that that monkey-generated power remains consistent at least under different external viscous environments.

We have also observed that power predictions remain reliable and consistent under different external viscous environments irrespective of the environmental condition of training data-set (Fig. 2(B)). We found similar results for speed (Fig. 2(C)) and other kinematic variables like joint position and velocity (not shown here). On the other hand, we noticed improved force prediction performance in the environments with higher gain fields than those of training data-set ($p<0.05$) but poorer prediction performance in the low gain field compared to training data ($p<0.001$, Fig. 2(A)). We believe that this is due to the fact that inverse dynamics has been used for calculations of kinetic variables, leading to minute inaccuracies in the derived force variable. Under high gain field conditions increased force generation leads to improved signal-to-noise ratio (SNR), where signal can be seen as generated force and the signal-independent noise as numerical inaccuracies associated with such derivation of force, and thus improved force predictions.
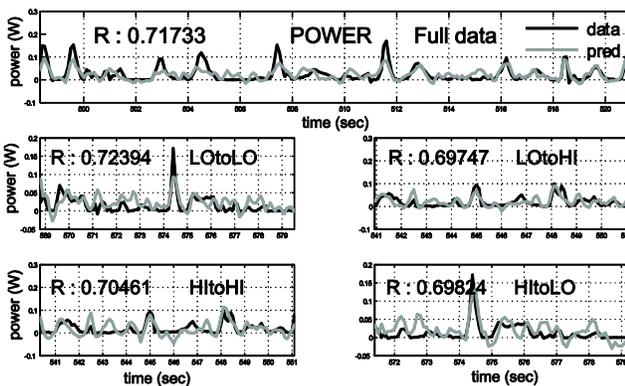

Fig. 3. Comparison of measured (dark) and predicted (light) power under different gain field conditions for models trained under different gain fields, using the same data set as shown in Fig. 1. Note that power prediction accuracies remain comparable unlike force (not shown) which we found to differ when the external environmental properties change. Refer to Fig. 2 for abbreviations used here.

These results favor the possibility of using force related variables, such as power, for controlling BMIs under different dynamical environments. Unlike kinematic variables, power contains the kinetic information of the movement; therefore, power might give users superior control over a prosthetic device. Using a dynamics related parameter such as power that incorporates kinematic and force information should allow for more natural BMI control and prove invaluable while working under differing dynamical conditions. Such force related control is also very important for writing on the chalkboard or driving the robotic arm under environmental boundary conditions like stiff wall etc. to prevent potential damage caused by limitations of kinematic controllers. This might make such

dynamics-related control a superior choice over traditional kinematics-based BMI algorithms. Further experiments are needed to demonstrate similar findings under a variety of dynamic environments. We are presently working on having the animals working against a continuum of different weight objects to be transported and various static and dynamic force field conditions. Such experiments should give us comprehensive insights to force and power distribution patterns and more thoroughly interpret the results we have presented here.

REFERENCES

[1] S. Musallam, B. D. Corneil, B. Greger *et al.*, "Cognitive control signals for neural prosthetics," *Science,* vol. 305, no. 5681, pp. 258-62, Jul 9, 2004.
[2] R. A. Andersen, J. W. Burdick, S. Musallam *et al.*, "Cognitive neural prosthetics," *Trends Cogn Sci,* vol. 8, no. 11, pp. 486-93, Nov, 2004.
[3] J. K. Chapin, K. A. Moxon, R. S. Markowitz *et al.*, "Real-time control of a robot arm using simultaneously recorded neurons in the motor cortex," *Nat Neurosci,* vol. 2, no. 7, pp. 664-70, Jul, 1999.
[4] J. Wessberg, C. R. Stambaugh, J. D. Kralik *et al.*, "Real-time prediction of hand trajectory by ensembles of cortical neurons in primates," *Nature,* vol. 408, no. 6810, pp. 361-5, Nov 16, 2000.
[5] D. M. Taylor, S. I. Tillery, and A. B. Schwartz, "Direct cortical control of 3D neuroprosthetic devices," *Science,* vol. 296, no. 5574, pp. 1829-32, Jun 7, 2002.
[6] M. D. Serruya, N. G. Hatsopoulos, L. Paninski *et al.*, "Instant neural control of a movement signal," *Nature,* vol. 416, no. 6877, pp. 141-2, Mar 14, 2002.
[7] J. M. Carmena, M. A. Lebedev, R. E. Crist *et al.*, "Learning to control a brain-machine interface for reaching and grasping by primates," *PLoS Biol,* vol. 1, no. 2, pp. E42, Nov, 2003.
[8] J. C. Sanchez, B. Mahmoudi, J. DiGiovanna *et al.*, "Exploiting co-adaptation for the design of symbiotic neuroprosthetic assistants," *Neural Netw,* vol. 22, no. 3, pp. 305-15, Apr, 2009.
[9] Z. Danziger, A. Fishbach, and F. Mussa-Ivaldi, "Learning Algorithms for Human-Machine Interfaces," *IEEE Trans Biomed Eng*, Feb 6, 2009.
[10] H. K. Kim, J. M. Carmena, S. J. Biggs *et al.*, "The muscle activation method: an approach to impedance control of brain-machine interfaces through a musculoskeletal model of the arm," *IEEE Trans Biomed Eng,* vol. 54, no. 8, pp. 1520-9, Aug, 2007.
[11] V. S. Chib, M. A. Krutky, K. M. Lynch *et al.*, "The separate neural control of hand movements and contact forces," *J Neurosci,* vol. 29, no. 12, pp. 3939-47, Mar 25, 2009.
[12] S. H. Scott, "Apparatus for measuring and perturbing shoulder and elbow joint positions and torques during reaching," *J Neurosci Methods,* vol. 89, no. 2, pp. 119-27, Jul 15, 1999.
[13] P. J. Rousche, and R. A. Normann, "Chronic recording capability of the Utah Intracortical Electrode Array in cat sensory cortex," *J Neurosci Methods,* vol. 82, no. 1, pp. 1-15, Jul 1, 1998.
[14] R. A. Normann, E. M. Maynard, P. J. Rousche *et al.*, "A neural interface for a cortical vision prosthesis," *Vision Res,* vol. 39, no. 15, pp. 2577-87, Jul, 1999.
[15] P. Y. Chhatbar, L. M. von Kraus, M. Semework *et al.*, "A bio-friendly and economical technique for chronic implantation of multiple microelectrode arrays," *J Neurosci Methods,* vol. 188, no. 2, pp. 187-94, May 15, 2010.
[16] D. L. Adams, J. R. Economides, C. M. Jocson *et al.*, "A biocompatible titanium headpost for stabilizing behaving monkeys," *J Neurophysiol,* vol. 98, no. 2, pp. 993-1001, Aug, 2007.

[17] M. A. Nicolelis, D. Dimitrov, J. M. Carmena *et al.*, "Chronic, multisite, multielectrode recordings in macaque monkeys," *Proc Natl Acad Sci U S A,* vol. 100, no. 19, pp. 11041-6, Sep 16, 2003.

[18] K. Fukunaga, *Introduction to statistical pattern recognition*: Academic Pr, 1990.

[19] A. H. Fagg, G. W. Ojakangas, L. E. Miller *et al.*, "Kinetic Trajectory Decoding Using Motor Cortical Ensembles," *Neural Systems and Rehabilitation Engineering, IEEE Transactions on,* vol. 17, no. 5, pp. 487-496, 2009.

[20] E. J. Cheng, and S. H. Scott, "Morphometry of Macaca mulatta forelimb. I. Shoulder and elbow muscles and segment inertial parameters," *J Morphol,* vol. 245, no. 3, pp. 206-24, Sep, 2000.

[21] D. W. Cabel, P. Cisek, and S. H. Scott, "Neural activity in primary motor cortex related to mechanical loads applied to the shoulder and elbow during a postural task," *J Neurophysiol,* vol. 86, no. 4, pp. 2102-8, Oct, 2001.

[22] I. Kurtzer, T. M. Herter, and S. H. Scott, "Random change in cortical load representation suggests distinct control of posture and movement," *Nat Neurosci,* vol. 8, no. 4, pp. 498-504, Apr, 2005.

[23] D. Nozaki, I. Kurtzer, and S. H. Scott, "Limited transfer of learning between unimanual and bimanual skills within the same limb," *Nat Neurosci,* vol. 9, no. 11, pp. 1364-6, Nov, 2006.

[24] D. Nozaki, and S. H. Scott, "Multi-compartment model can explain partial transfer of learning within the same limb between unimanual and bimanual reaching," *Exp Brain Res,* vol. 194, no. 3, pp. 451-63, Apr, 2009.

[25] A. P. Georgopoulos, J. Ashe, N. Smyrnis *et al.*, "The motor cortex and the coding of force," *Science,* vol. 256, no. 5064, pp. 1692-5, Jun 19, 1992.

[26] K. M. Graham, K. D. Moore, D. W. Cabel *et al.*, "Kinematics and kinetics of multijoint reaching in nonhuman primates," *J Neurophysiol,* vol. 89, no. 5, pp. 2667-77, May, 2003.

[27] I. Kurtzer, T. M. Herter, and S. H. Scott, "Nonuniform distribution of reach-related and torque-related activity in upper arm muscles and neurons of primary motor cortex," *J Neurophysiol,* vol. 96, no. 6, pp. 3220-30, Dec, 2006.

[28] R. Gupta, and J. Ashe, "Offline Decoding of End-Point Forces Using Neural Ensembles: Application to a Brain-Machine Interface," *Neural Systems and Rehabilitation Engineering, IEEE Transactions on,* vol. 17, no. 3, pp. 254-262, 2009.